



Cite this: *Nanoscale Adv.*, 2023, **5**, 3131

Received 29th November 2022  
Accepted 16th February 2023

DOI: 10.1039/d2na00866a  
[rsc.li/nanoscale-advances](http://rsc.li/nanoscale-advances)

## Recent progress in flexible micro-pressure sensors for wearable health monitoring

Jianguo Hu, Guanhua Dun, Xiangshun Geng, Jing Chen, Xiaoming Wu and Tian-Ling Ren\*

In recent years, flexible micro-pressure sensors have been used widely in wearable health monitoring applications due to their excellent flexibility, stretchability, non-invasiveness, comfort wearing and real-time detection. According to the working mechanism of the flexible micro-pressure sensor, it can be classified as piezoresistive, piezoelectric, capacitive and triboelectric types. Herein, an overview of flexible micro-pressure sensors for wearable health monitoring is presented. The physiological signaling and body motions contain a lot of health status information. Thus, this review focuses on the applications of flexible micro-pressure sensors in these fields. Additionally, the contents of sensing mechanism, sensing materials and performance of flexible micro-pressure sensors are introduced in detail. Finally, we predict the future research directions of the flexible micro-pressure sensors, and discuss the challenges in practical applications.

## 1 Introduction

With the continuous improvement of people's living standards, considerable attention has been paid to physical health. Moreover, people's investment in health-related devices is strongly increasing and has attracted a large number of scientific and technological personnel to develop wearable health monitoring equipment.<sup>1–21</sup> In order to meet people's needs for health monitoring and medical diagnosis, many researchers have proposed and developed a variety of wearable electronic devices and electronic skin devices.<sup>22–36</sup> As a main part of wearable electronic devices, the wearable health monitoring system based on flexible micro-pressure sensors is a focal developmental direction and solution strategy. It should be noted that the micro-pressure sensors in this review refer to sensors, which can detect small pressure signals, not the small size of the pressure sensor.

In recent years, cardiovascular diseases have become one of the leading causes of death around the world.<sup>37</sup> According to the forecasts of the relevant institutions, the number of human deaths caused by cardiovascular diseases will exceed 23.6 million in 2030.<sup>38</sup> Common cardiovascular diseases include coronary heart disease, arrhythmia, hypertension and cardiomyopathy,<sup>39–44</sup> considering that these diseases are closely related to physiological signaling such as heartbeat, blood pressure and pulse waves. Therefore, the wearable pressure sensors for monitoring of physiological signaling can be used to

observe and effectively predict cardiovascular diseases.<sup>45–48</sup> Except the physiological signals, the body motions such as eye blinking, finger and wrist bending and muscle motion are also closely related to body health.<sup>49–56</sup> Currently, the wearable pressure sensors have been combined with artificial intelligence and new materials, constantly developing in the direction of intelligence, miniaturization and flexibility. Furthermore, they are more comfortable to wear and can monitor the physiological signals of the body for a long time. These advantages of flexible wearable pressure sensors may facilitate solving the needs of personalized health care.<sup>57,58</sup>

Heartbeat and pulse waves are the main components of human physiological signaling,<sup>59,60</sup> and contain a lot of personal health information, such as heart status and blood pressure. A variety of flexible micro-pressure sensors for monitoring the heartbeat and pulse waves have been developed.<sup>61–66</sup> Compared to the photoplethysmography measurement method, the flexible micro-pressure sensors can realize continuous and real-time monitoring for pulse waves.<sup>67–69</sup>

The organs and tissue motion also reflect the state of the human body.<sup>70–72</sup> For example, the eye blinking condition is able to predict eye fatigue.<sup>73</sup> The status of finger bending and wrist joint movement show the health condition of normal function of the human body.<sup>74,75</sup> The muscle motions are also closely related to body health.<sup>76</sup> Currently, many researchers have developed a lot of flexible micro-pressure sensors for monitoring conditions of eye and organ movement.<sup>77–80</sup> These sensors significantly help people by monitoring their health status in real-time.

Flexible electronic devices based on 2D materials have developed into one of the most promising fields for next-

School of Integrated Circuits, Beijing National Research Center for Information Science and Technology (BNRist), Tsinghua University, Beijing 100084, China. E-mail: [rentl@tsinghua.edu.cn](mailto:rentl@tsinghua.edu.cn)



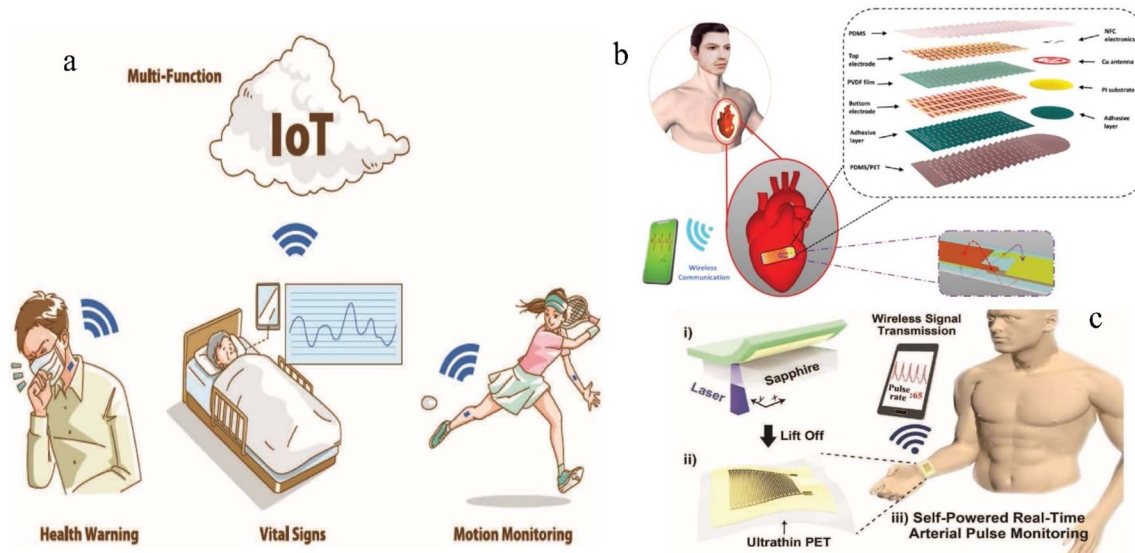


Fig. 1 Applications of flexible micro-pressure sensors for wearable health monitoring. (a) Multifunctional materials and composites for health monitoring.<sup>91</sup> (b) Schematic illustration of the integrated device with multilayered structures between two subsystems: the stretchable sensor and wireless patch, and enlarged electrode patterns.<sup>92</sup> (c) Schematic illustration of the fabrication process for self-powered pressure sensor.<sup>203</sup> Reproduced with permission. Figure (a) has been adapted/reproduced from ref. 91 with permission from Wiley-VCH GmbH, copyright 2022. Figure (b) has been adapted/reproduced from ref. 92 with permission from Wiley-VCH Verlag GmbH & Co. KGaA, Weinheim, copyright 2019. Figure (c) has been adapted/reproduced from ref. 203 with permission from Wiley-VCH Verlag GmbH & Co. KGaA, Weinheim, copyright 2017.

generation electronics because of their flexibility, stretchability and integration.<sup>81–83</sup> As a major component of flexible electronic devices, the flexible micro-pressure sensors have become a key research direction. Considering that the flexible micro-pressure sensors can be integrated easily into portable mobile devices to detect the micro-local pressure,<sup>84</sup> the flexible micro-pressure sensors can thus be used easily and widely in wearable health monitoring.<sup>85–90,199–202</sup> Fig. 1 shows the applications of flexible micro-pressure sensors for wearable health monitoring. In this review, we describe in detail the development process of the flexible micro-pressure sensors, summarize the current research status of the flexible micro-pressure sensors in wearable health monitoring, and also predict the future research directions of the flexible micro-pressure sensors. This review will greatly improve the understanding of researchers in scientific community, and contribute to the development of flexible micro-pressure sensors. In addition, it will significantly promote the cross-research of the flexible micro-pressure sensors and other scientific fields.

## 2 Sensing mechanisms of flexible micro-pressure sensors

Sensing mechanisms reveal the working modes of flexible micro-pressure sensors. According to the sensing mechanisms, the pressure sensors can be classified into four types: piezoresistive sensors,<sup>93–95</sup> capacitive sensors,<sup>96–99</sup> piezoelectric sensors<sup>100,101</sup> and triboelectric sensors.<sup>102,103</sup> Generally speaking, the most commonly used sensing mechanisms in wearable health monitoring devices are the piezoresistive, capacitive and

piezoelectric. Additionally, the external power supply system is indispensable for piezoresistive and capacitive pressure sensors, and these two types of sensors are often used in static excitation.<sup>104–107</sup> However, piezoelectric and triboelectric pressure sensors can be self-powered, and they are suitable used in dynamic excitation.<sup>108–112</sup> Finally, these sensing mechanisms are described in detail as follows. It is worth noting that the performance of the flexible pressure sensor is determined by its functional material and microstructure.

### 2.1 Piezoresistive micro-pressure sensors

The sensing mechanism of the piezoresistive micro-pressure sensor is material piezoresistive effect. Namely, the corresponding resistance of the sensor will change due to applying pressure on the sensor surface. Fig. 2(a) shows the sensing mechanism of the piezoresistive pressure sensors. The piezoresistive micro-pressure sensor has been used widely because it has a simple structure, a convenient method of measurement, large measurement range and low energy consumption. It is well known that the resistance of the conductor can be calculated by the following equation:<sup>113,115</sup>

$$R = \frac{\rho L}{A} \quad (1)$$

where  $\rho$  is the conductor resistivity;  $L$  and  $A$  present the conductor length and the conductor cross-sectional area, respectively. Considering the strain sensor of the piezoresistive type, the change of resistance can be described as:

$$\frac{\Delta R}{R} = (1 + 2\nu)\varepsilon + \frac{\Delta \rho}{\rho} \quad (2)$$



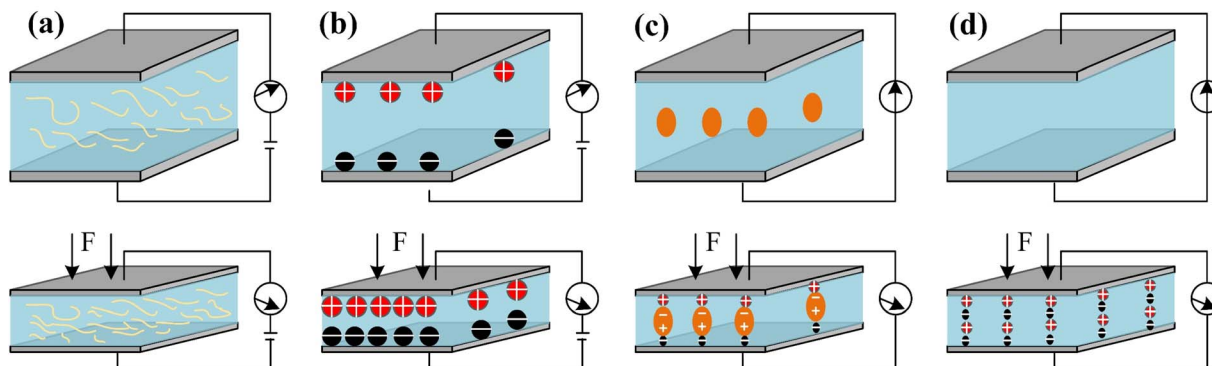


Fig. 2 Sensing mechanisms of the pressure sensors. (a) Piezoresistive type; (b) capacitive type; (c) piezoelectric type; (d) triboelectric type.

where  $\varepsilon$  is the Poisson strain and  $v$  is the Poisson ratio. It should be noted that the resistance change of the piezoresistive pressure sensor originates mainly from its geometry change and the contact resistance between the electrode and the materials. The change of materials in the energy band structure also leads to its piezoresistivity change. This piezoresistivity change derives from the change in band-gap because of the external press.

The quantum tunnelling effect of the conductive composites is also closely related to the piezoresistive mechanism. The common conductive composites are fabricated by mixing nanoparticles and polymers, and it leads to the formation of a tunnelling barrier between the nanoparticles and polymeric layer. Therefore, the piezoresistive mechanism caused by the quantum tunnelling effect of the conductive composites can be described as follows. When the piezoresistive sensor based on conductive composites is derived from an external press, mechanical deformation occurs. It induces a decrease in the thickness of the polymeric layer so that a decrease in the tunnelling barrier occurs. Then, a reduction of the composite resistance will appear. In this process, the piezoresistive press sensors are developed.

## 2.2 Capacitive micro-pressure sensors

The sensing mechanism of the capacitive micro-pressure sensor is to convert pressure into the change of capacitance. The capacitance changes lead to changes in electrical signals. In general, the capacitive micro-pressure sensor is made up of a parallel-plate capacitor, which consists of two parallel electrodes and a dielectric layer. Fig. 2(b) shows the sensing mechanism of the capacitive micro-pressure sensor. The principle of the capacitive micro-pressure sensor can be described as follows:<sup>114</sup>

$$C = \frac{\varepsilon S}{4\pi k d} \quad (3)$$

where  $\varepsilon$  is the relative dielectric constant;  $k$  is the electrostatic force constant;  $S$  is the overlap area of two parallel plates; and  $d$  is the distance of two parallel plates. This equation shows the parameters of the relative dielectric constant. The overlap area and the distance are sensitive to pressure changes. In practical applications, the change in the distance parameter of the pressure sensor is typically used, such as measuring share

forces and strain. The change in the parameter of the relative dielectric constant has not been widely used because this type of sensor requires special material design. The shear stress can also be detected by changing the parameter of the overlap area.

According to the working mechanism of the capacitive micro-pressure sensor, it is well known that the press sensitivity of the sensor is decided by the compressibility of the dielectric materials. Therefore, the capacitive micro-pressure sensors with excellent performance can be designed by using the dielectric of high compressibility. For example, the performance of tactile sensors can be improved significantly by using the structure of porous dielectric layers due to its high compressibility.<sup>115–117</sup>

## 2.3 Piezoelectric micro-pressure sensors

The piezoelectric micro-pressure sensor has been widely used in wearable health monitoring, and its working mechanism is the piezoelectricity of the material. This working mechanism also can be called the piezoelectric effect. Specifically, the piezoelectric effect of the material is a kind of macroscopic polarization phenomenon caused by external pressure. The charge amount on the electrode surface can be calculated by:<sup>118</sup>

$$Q = d_{33} \times A \times F \quad (4)$$

where  $d_{33}$  is the piezoelectric constant, 33 means that the direction of pressure is consistent with the direction of polarization;  $A$  is the electrode area; and  $F$  is the external pressure. The sensor developed by the piezoelectric effect of the material means that it has the ability to convert the external pressure into an electrical signal. Fig. 2(c) shows the working mechanism of the piezoelectric micro-pressure sensor.

Considering the working mechanism of the piezoelectric sensor, it can be used as a nanogenerator because it has the ability to harvest vibrational energy and it converts mechanical energy into electric energy. Therefore, it is often used as the energy supply part of wearable electronic devices. The main part of the flexible piezoelectric micro-pressure sensor is the piezoelectric film and flexible substrate. Polyvinylidene-fluoride (PVDF) is a common flexible piezoelectric material, and it can manufacture the flexible piezoelectric film.<sup>119,120</sup>



## 2.4 Triboelectric micro-pressure sensors

The triboelectric effect describes the phenomenon in which the electrical charges occur on the material surface under the condition that two different material layers are rubbed with each other.<sup>121</sup> It is obvious that the working mechanism of the triboelectric micro-pressure sensor is based on the triboelectric effect of the material. Generally speaking, triboelectric nanogenerator pressure sensors are based on the coupling effect of friction electrification and electrostatic induction, which is an effective way to convert human mechanical energy into electric energy and realize self-powered wearable sensors.<sup>122-124</sup> Fig. 2(d) shows the working mechanism of triboelectric micro-pressure sensor. Considering that the amounts of triboelectric charge are affected by many factors, such as environmental humidity, external pressure, and environmental temperature, it is thus very hard to develop a single variable condition for the triboelectric micro-pressure sensor to sense pressure in practical applications.

## 3 Recent advances of piezoresistive micro-pressure sensors for wearable health monitoring

Flexible piezoresistive micro-pressure sensors have promising applicable potential because of their simple structure, facile materials preparation, low cost, and other merits.<sup>125-127</sup> Graphene, carbon nanofibers and carbon nanotubes (CNTs) are the most common conductive materials for preparing piezoresistive pressure sensors.<sup>128</sup> These sensors have high sensitivity, great stretchability, good flexibility, and excellent stability, and are suitable for micro-pressure detection in different application scenarios.<sup>129-131</sup>

### 3.1 Piezoresistive materials

In piezoresistive materials, the piezoelectric effect always exists for the preparation of wearable devices. Carbon materials with specific structures, such as carbon fibrous sponges and carbon nanofibers, are the most common piezoresistive materials. Gao *et al.* fabricated the carbon fibrous sponges,<sup>132</sup> and the fabrication procedure is shown in Fig. 3. The PI membrane is mechanically cut into short PI fibres and soaked in polyurethane solution. After being GO-coated, the sample was freeze-dried for 48 hours, and named as PIPUGO SF. To obtain a PIPUGO sponge, PIPUGO SFs was dispersed in dioxane and freeze-dried for 48 h. The carbon fibrous sponges were obtained by thermal treatment. The polypyrene role can also be used to achieve piezoresistive effects. Li *et al.* developed an efficient strategy to greatly improve the pressure resistance performance by using PDMS micro-pyramids.<sup>133</sup> To meet the requirements of pressure sensing,  $Ti_3C_2T_x$  MXene,<sup>134</sup> silver nanowire/PEDOT:PSS/polyimide aerogels<sup>135</sup> were selected to serve as piezoresistive materials to construct high-performance pressure sensors.

### 3.2 Physiological monitoring

Flexible electronics can realize wearable physiological signal monitoring on human skin surfaces, which has become

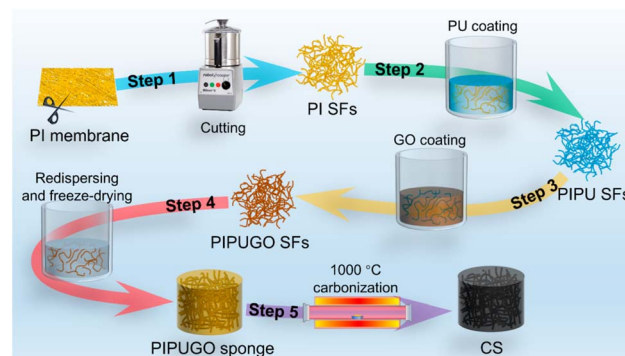


Fig. 3 The fabrication procedure of carbon fibrous sponges.<sup>132</sup> Reproduced with permission. Figure has been adapted/reproduced from ref. 132 with permission from American Chemical Society, copyright 2022.

a revolutionary science and technology in sports health management, disease diagnosis and monitoring, environmental monitoring, human-computer intelligent interaction and other fields, as well as an important strategic emerging industry in various countries. Human physiological signals include pulse beating, heart beating, respiration and other signals. In the past decade, different kinds of piezoresistive sensors have been studied for physiological signal monitoring. Liu *et al.* presented a high-performance piezoresistive flexible pressure sensor for human health monitoring based on wrinkled microstructures.<sup>136</sup> Fig. 4 shows the pressure sensor for extensive human physiological monitoring.

To improve the performance of the sensors, a pyramid structure and porous structure have been developed. For example, a high sensitivity near  $2000 \text{ kPa}^{-1}$  and an ultralow

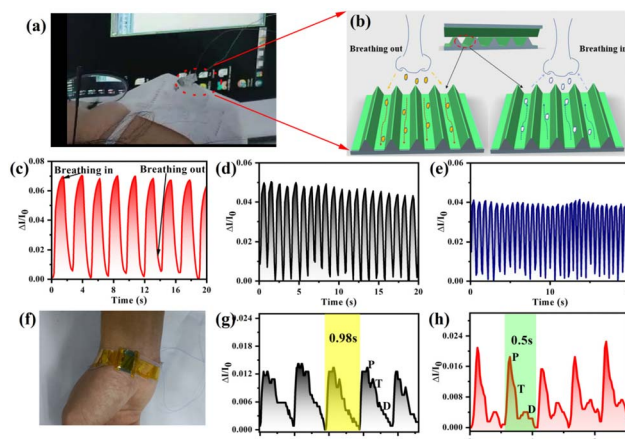


Fig. 4 The PPF@PDMS pressure sensor for extensive human movement monitoring. (a) Signal of the finger periodically pressing the sensor. (b) Signal waveform of a single period. (c) Response and recovery times for a single press. (d) Response signal for finger bending to 01, 301, 451, 601 and 901 in sequence. (e) Response signal for cyclic finger bending to 601. (f) Response signal for elbow bending to 601. (g and h) Response signal for accelerated walking.<sup>136</sup> Reproduced with permission. Figure has been adapted/reproduced from ref. 136 with permission from The Royal Society of Chemistry 2022, copyright 2022.



detection limit (0.075 Pa) were realized using a short channel length and sharp micropyramids.<sup>133</sup>

### 3.3 Motion monitoring

With the improvement of living standards and the development of sports, more people are participating in sports. Some extreme sports have also gradually become popular means of mass fitness. Ma *et al.*<sup>137</sup> developed a piezoresistive pressure sensor by coating MXene flakes with different degrees of *in situ* oxidation onto paper substrates. Its sensitivity and detection limit reached  $28.43 \text{ kPa}^{-1}$  and 0.8 Pa, respectively. Moreover, it can track body movements such as elbow movement and finger tapping. Yuan *et al.* improved the sensitivity to  $11\,668.6 \text{ kPa}^{-1}$  and reduced the detection limit to as low as 0.425 Pa by simultaneously modulating the body resistance and the contact resistance.<sup>129</sup> Subsequently, Park *et al.* achieved ultrahigh sensitivity of up to  $3.8 \times 10^5 \text{ kPa}^{-1}$  using carbonaceous protrusions by laser annealing on a CNT layer. The high sensitivity was attributed to the extremely low initial current and high current under an external pressure.<sup>138</sup>

Generally, it is difficult for conventional piezoresistive pressure sensors to achieve both high sensitivity and a wide pressure range. In 2021, Wang *et al.* proposed a new  $\text{Co}_3\text{O}_4$ /carbon felt pressure sensor.  $\text{Co}_3\text{O}_4$  provides a low initial current without loading and carbon felt provides a high output current under loading, which extends the measurement range of the pressure sensors. The fabricated pressure sensors exhibit high sensitivity ( $243 \text{ kPa}^{-1}$ ) and a broad range (up to 180 kPa) of measurements.<sup>139</sup>

## 4 Recent advances of capacitive micro-pressure sensors for wearable health monitoring

A typical capacitive pressure sensor includes a dielectric layer and electrodes on both sides. The sensor will deform when the pressure/strain is applied, causing the change of capacitance, thus completing the transformation of the pressure signal to the electrical signal. The high sensing performance includes good sensitivity, wide response range, low detection limit, and fast response time. Comparing the other types (piezoresistive, piezoelectric and triboelectric) of pressure sensors, the capacitive pressure sensor has some advantages in rapid dynamic response, temperature insensitivity and low power consumption.<sup>140</sup> Therefore, the capacitive pressure sensors have attracted much attention for use in health monitoring. Fig. 5 shows the main applications of capacitive pressure sensors.

### 4.1 Pulse wave monitoring

Blood pressure is a crucial sign of good health. Bao *et al.* reported a single-use biodegradable pressure sensor patch to detect the pulse wave, and the sensitivity of the sensor is very high ( $0.76 \text{ kPa}^{-1}$ ).<sup>143</sup> To obtain high-sensing performance sensors, various strategies have been proposed. Atalay *et al.* investigated the influence of soft conductive fabric types and

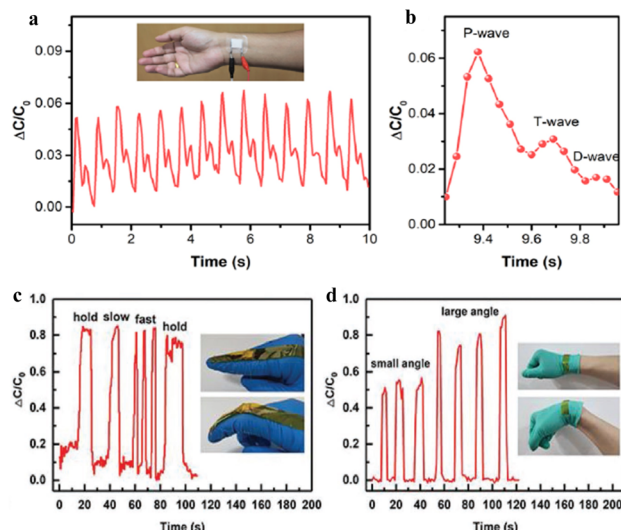


Fig. 5 The main application of capacitive sensors, (a) and (b) are pulse wave monitoring.<sup>141</sup> (c) and (d) are finger and wrist bending.<sup>142</sup> Reproduced with permission. Figure (a and b) has been adapted/reproduced from ref. 141 with permission from American Chemical Society, copyright 2020. Figure (c and d) has been adapted/reproduced from ref. 142 with permission from Wiley-VCH GmbH, copyright 2021.

sacrificial particle types on the sensing behaviors of pressure sensors. It was found that a high dielectric porosity and conductive knit electrode are beneficial to obtaining a high sensing performance. This provides guidance for a high-performance sensor design.<sup>144</sup> Jang *et al.* achieved a high-performance sensor by increasing the dielectric properties of elastomers. The authors designed the dielectric properties of elastomers using multi-walled carbon nanotube (MWCNT)/polydimethylsiloxane (PDMS), where the MWCNT is modified by alkylamine. Due to the enhanced dielectric constant of the composite compared with pure PDMS, the as-fabricated sensor shows improved sensing performance.<sup>145</sup> Guo *et al.* obtained a capacitive pressure sensor using poly (vinylidenefluorideco-trifluoroethylene) [P(VDF-TrFE)] dielectric film combined with nanopillars on both sides. The addition of nanopillars enabled a good sensitivity of  $0.35 \text{ kPa}^{-1}$ , a working range of from 4 Pa to 25 kPa, and a high response time of less than 48 ms.<sup>146</sup>

The design of three-dimensional (3D) structures also contributes to higher sensing performance. Zhao *et al.* demonstrated a 3D structure to obtain improved sensing property, where the TPU/Ag nanowire network was designed. A high sensitivity of up to  $1.21 \text{ kPa}^{-1}$  was acquired, which enabled good figure pressure sensing behaviors.<sup>140</sup> Li and co-workers reported a wide range sensor based on the high porosity elastomeric dielectric layer. The conducting polymer/filter paper electrodes were used to form a sandwiched capacitive sensor structure.<sup>76</sup> Ma *et al.* presented a micro-arrayed PMDS-based high sensitivity pressure sensor. Ag nanowires were used as the top and bottom electrodes. This device has a high sensitivity of  $2.04 \text{ kPa}^{-1}$ , and low pressure ranges of 0–2000 Pa.<sup>147</sup> Park *et al.* demonstrated a porous Ecoflex-based capacitive sensor



using a simple melting process. The electrode layers are each based on carbon fiber thin films and polydimethylsiloxane-based silver nanowires. The as-fabricated sensors show a high sensitivity of  $0.161 \text{ kPa}^{-1}$  for low pressure ( $<10 \text{ kPa}$ ) and a wide range of  $<200 \text{ kPa}$ , and a good durability ( $>6000$  cycles).<sup>148</sup> Luo *et al.* demonstrated a pressure sensor with a tilted micropillar array enhanced dielectric layer. The tilted micropillars show potential for bending rather than compression deformation. Thus, it is easy to vary the distance between the electrodes. This is beneficial for obtaining high sensitivity and a small detection limit.<sup>149</sup>

#### 4.2 Motion monitoring

Recently, capacitive pressure sensors have been widely used in motion monitoring due to their excellent performance. Wu *et al.* fabricated a capacitive pressure sensor with extraordinary sensitivity and wide sensing range using a PAM/BIS/GO nanocomposite hydrogel to detect body motions such as elbow bending and knee bending.<sup>150</sup> Sun *et al.* proposed a PDMS microbeads-modified dielectric layer for a flexible capacitive pressure sensor to achieve high sensitivity ( $0.048 \text{ kPa}^{-1}$ ) in the range of  $0\text{--}10 \text{ kPa}$ , and it was successfully applied to detect finger and wrist bending.<sup>142</sup>

Inspired by biological structures such as lotus leaves and roses, there is hope to design pressure sensors with higher performance. Wan and co-workers presented a tactile sensor based on polydimethylsiloxane (PDMS) with low-density micro towers and a high-aspect ratio. The *m*-PDMS was designed to form a bionic micropattern that replicates the lotus leaf. The silver nanowires are used as bottom electrodes. This sensor shows a good sensitivity of  $\approx 1.2 \text{ kPa}^{-1}$ , a low detection limit ( $<0.8 \text{ Pa}$ ), and a fast response time (36 ms).<sup>77</sup> Moreover, Mahata *et al.* demonstrated a pressure sensor using the single/double layer well-designed PDMS and indium tin oxide (ITO) electrodes. The sensor mimics the rose petals with the hemisphere including micropapillary and nano-folds, and has a high sensitivity of  $0.055 \text{ kPa}^{-1}$  over a wide range of 0.5 to 10 kPa with a response time that is lower than 200 ms.<sup>151</sup>

In addition to the higher sensing characteristics, degradability is a design key for capacitive stress sensors. Bouthry *et al.* reported a strain and pressure sensor with well-designed POMaC top encapsulation layers, which exhibits high sensitivity and a fast response time. Importantly, these sensors have good biodegradability, which may enable their biomedical applications, including orthopedic applications.<sup>152</sup>

## 5 Recent advances of piezoelectric micro-pressure sensors for wearable health monitoring

In recent years, as people pay more attention to their own health, health monitoring based on piezoelectric micro-pressure sensors has been developing rapidly.<sup>21,91</sup> In general, the health monitoring consists of physiological signals and motion detection. Currently, there are increasingly more materials with piezoelectricity that have been found or synthesized.<sup>91</sup> The most common

piezoelectric materials include lead zirconate titanate (PZT) and polyvinylidene fluoride (PVDF).<sup>21</sup> Moreover, some new piezoelectric materials have been developed; for example, piezoelectric bio-electronic-skin and gallium nitride thin film.<sup>153</sup> Considering the integrated development of artificial intelligence and health monitoring, new bio-intelligent piezoelectric materials will continue to appear in the future. The application of piezoelectric sensors in the field of health monitoring is mainly reflected in the following aspects: heart monitoring, pulse monitoring, eye monitoring, gait monitoring, joint monitoring and other areas.<sup>91</sup>

#### 5.1 Piezoelectric materials

The piezoelectric effect is a special property of materials, and not every material has the piezoelectric effect. A piezoelectric material is an important part of the piezoelectric sensor. Conventionally, lead zirconate titanate (PZT), polyvinylidene fluoride (PVDF) and barium titanate ( $\text{BaTiO}_3$ ) are the most used piezoelectric materials. Currently, with the development of flexible electronic technology, more flexible piezoelectric micro-pressure sensors have been reported. Generally speaking, the flexible piezoelectric sensor is realized by making the piezoelectric material on the flexible substrate material. Polydimethylsiloxane (PDMS) is commonly used as a flexible substrate material. Table 1 shows the piezoelectric materials that are used in micro-pressure sensors. Furthermore, in order to meet the practical needs of miniaturization, intelligence and integration, new piezoelectric materials that can be used to make piezoelectric micro-pressure sensors for health monitoring will continue to be developed.

#### 5.2 Heart monitoring

The heart is one of the most important organs in the body. Every year, millions of people die from heart diseases around the world. Therefore, real-time monitoring of the heart is a very important solution to find heart problems and prevent death. In the past, most of the piezoelectric sensors lacked stretchability and flexibility due to the limitations of the piezoelectric materials used, which led to the lack of application in human health monitoring. Currently, with the development of flexible piezoelectric materials, many flexible piezoelectric health monitoring systems have emerged.

The status of a pulse is one crucial indicator of heart health. It also can be used to analyze the heart rate and heartbeat. Because of the strong pulse in the wrist and neck of the human body, it is often used as two key positions for pulse detection based on the piezoelectric micro-pressure sensor attached to the wrist and neck for real-time pulse detection. Shi *et al.* designed a piezoelectric micro-pressure sensor based on 1-layer of LDPE/Teflon AF piezo-electret to detect the low pressure signal of the human pulse.<sup>159</sup> In order to acquire the low-pressure signal of the pulse wave, they utilized a current amplifier to amplify the pulse signal and designed a data acquisition system based on a personal computer. This piezoelectric micro-pressure sensor was realized to measure the pulse beat on the waist hand.



Table 1 Parameters of common piezoelectric materials

Materials	Polling (kV cm <sup>-1</sup> )	$d_{31}$ (pm V <sup>-1</sup> )	$d_{33}$ (pm V <sup>-1</sup> )	$g_{31}$ (0.001 V mN <sup>-1</sup> )	$g_{33}$ (0.001 V mN <sup>-1</sup> )	$\varepsilon_r$
Lead-PZT <sup>154</sup>	60	50	200–400	11	25–35	500
PLZT <sup>155,156</sup>	12.4	–262	710	—	22.2	2214
Lead-free PVDF <sup>154</sup>	—	8–22	10–15	—	70–170	6–12
P(VDF-TrFE) <sup>157</sup>	15–30	12	–38	—	—	18
PDMS <sup>158</sup>	—	—	1645 pC N <sup>-1</sup>	—	—	—
FEP <sup>158</sup>	—	—	5400 pC N <sup>-1</sup>	—	—	—
LDPE <sup>159</sup>	—	—	1100 pC N <sup>-1</sup>	—	—	—
Polypropylene (PP) <sup>160</sup>	—	—	600 pC N <sup>-1</sup>	—	—	—
BaTiO <sub>3</sub> (ref. 161)	2	–33.4	190	1.89	11.87	1200
KNN <sup>162</sup>	5	–51	127	–11.6	29	496
GaN <sup>163,164</sup>	—	–1.9	3.7	—	—	8.58

Chu *et al.* designed an active and flexible pulse wave sensing system based on a fluorinated propylene (FEP)/Ecoflex/FEP piezoelectric micro-pressure sensor for detecting the pulse wave.<sup>165</sup> They designed a piezo-electret sensing system for pulse wave detection, as shown in Fig. 6. The experimental results show that this sandwich-structured piezo-electret has a high sensitivity of 32.6 nA kPa<sup>-1</sup> and an excellent piezoelectric coefficient  $d_{33}$  value of up to 4100 pC N<sup>-1</sup>. It is the ultra-high piezoelectric coupling performance of the designed

piezoelectric sensor that enables it to accurately distinguish the pulse waveforms and characteristics of different participants.

Fig. 6(b) shows an implantable flexible wireless piezoelectric micro-pressure sensor for heart monitoring. Sun *et al.* developed a flexible and stretchable integrated sensing system based on the piezoelectric pressure sensor to realize heart monitoring. This sensing system uses malleable PVDF films and PDMS substrates to achieve excellent ductility and flexibility. Additionally, this system is self-powered, and the power reaches a maximum of 228 nW under a load resistance of 68 MΩ.<sup>92</sup>

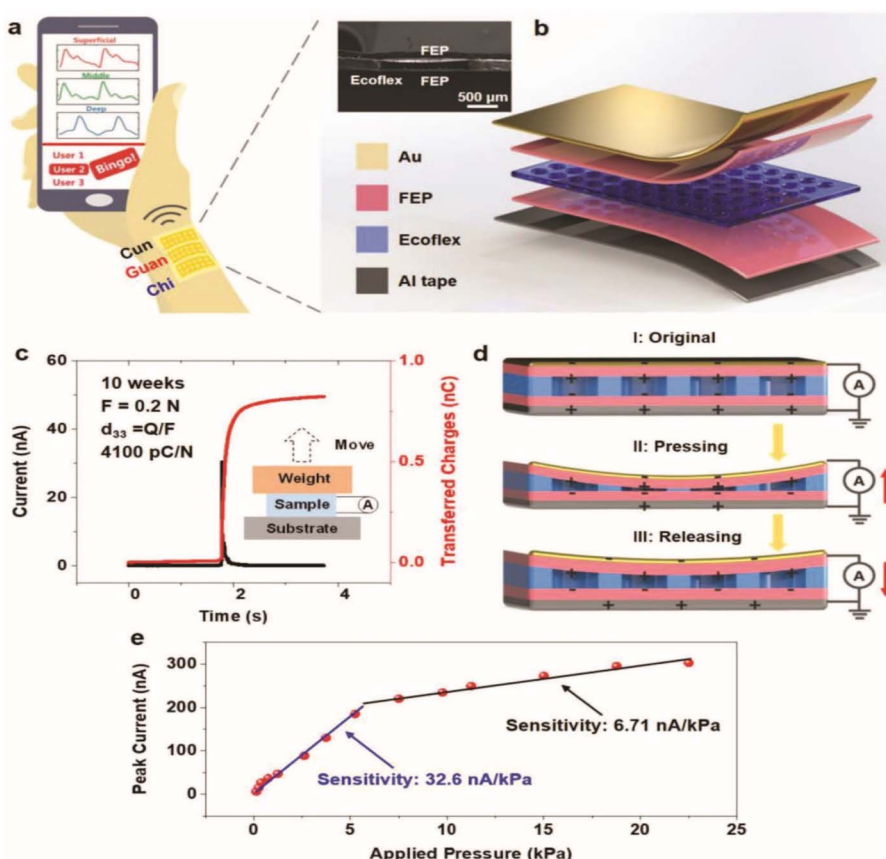


Fig. 6 Triboelectric micro-pressure sensors for pulse waves detection.<sup>165</sup> (a) M-Health system concept. (b) The schematic diagram of the pulse sensing device. (c) Equivalent piezoelectric coefficient measurement. (d) The working process of a pulse wave sensor. (e) Peak short-circuit currents and sensitivity of a typical pulse sensor. Reproduced with permission. Figure has been adapted/reproduced from ref. 165 with permission from Wiley-VCH Verlag GmbH & Co. KGaA, Weinheim, copyright 2018.



Samartkit developed a non-invasive heart rate and blood pressure monitoring system based on a PZT piezoelectric and photoplethysmographic sensor, and presented a modified pulse transit time technique to demodulate the time delay.<sup>166</sup> The experimental results showed that this system reaches an accuracy range of 93.33% (with respect to a reference device) of all heart rate measurements.

### 5.3 Motion monitoring

The movement of the human body and the activity of each joint is an important reflection of human health. Therefore, the monitoring of human movement and joints enables the monitoring of human health. The common means of monitoring body motion is eye motion, finger bending, wrist joint bending, and muscle motion. The main advantages in wearable piezoelectric pressure sensors are their non-invasiveness, convenience, flexibility, high sensitivity and real-time monitoring.

Eye health is an important part of human health. As people continue to look at electronic devices for a long time, there are an increasing number of eye problems. Thus, the monitoring of eye movement has great value. The most common eye problem is eye fatigue. Eye movements can reflect some health problems such as eye fatigue. Kim *et al.* developed a highly sensitive, non-invasive flexible piezoelectric sensor to detect the eye movement.<sup>167</sup> Eye movement is realized by attaching a flexible sensor on the skin near the eyes, and the movement of skin near the eye can lead to a change in the bending degree of the sensor. Additionally, this flexible sensor is attached to different parts of the eye to accomplish the detection of blinking, looking forward, looking left, looking right and other motions. Lü *et al.* designed a flexible piezoelectric sensor based on a Kapton substrate for monitoring eye fatigue, and presented a theoretical model to reveal the underlying mechanism of detecting eyelid motion.<sup>168</sup>

Finger bending and wrist joint movement are also important parts of the normal function of the human body. Fang *et al.* fabricated a flexible piezoelectric sensor to detect the hand and wrist movements, and recorded the force myography to realize body motion monitoring.<sup>169</sup> Moreover, they developed artificial neural network algorithms to classify the hand and wrist movements, and the average motion-classification accuracies of the hand and wrist movements reached 96.1 and 94.8%, respectively. Zhang *et al.* developed a flexible piezoelectric sensor based on ZnO nanorods attached onto a Cu-coated polyimide substrate. The sensor exhibits a high sensitivity of  $974 \text{ mV N}^{-1}$  and the wide linear range of 0.1–1 N, and it has been successfully used to monitor finger bending.<sup>170</sup>

## 6 Recent advances of triboelectric micro-pressure sensors for wearable health monitoring

Recently, triboelectric nanogenerators (TENGs) pressure sensors have been used widely in self-powered flexible wearable electronics for health monitoring due to its excellent performance in energy harvesting and sensing.<sup>171</sup> The triboelectric

micro-pressure sensor consists of a couple of triboelectric active layers and electrodes. According to friction electricity, the triboelectric micro-pressure sensor can be classified into four categories, which are lateral sliding mode, single electrode mode, contact separation mode and freestanding triboelectric layer mode. The application of pressure sensors based on TENGs somatosensory has great medical benefits for human, because it can convert the inexhaustible biomechanical energy such as blood circulation and muscle movement into electrical output, providing information that reflects the human physiological status. In health monitoring applications, triboelectric pressure sensors based on TENGs operate as both an energy collection device and an active sensor. The bioinspired triboelectric TENGs pressure sensors for self-powered wearable health monitoring also get rapid development.<sup>172</sup>

### 6.1 Triboelectric materials

The triboelectric effect is a phenomenon that can be observed in many materials. Thus, many materials can be used to fabricate triboelectric pressure sensors. However, not all materials with friction electrification are suitable for making triboelectric pressure sensors with high performance due to the different properties of the friction electrification of materials. According to results from related studies, carbon-based materials, composite conductive materials and polymer materials are commonly used in the manufacturing of high-performance flexible triboelectric pressure sensors.

Recently, carbon-based materials have been used widely in triboelectric pressure sensors based on TENGs. MXene has attracted much attention in sensor fields because of its unique electronic and mechanical properties. Yi *et al.* reported a self-powered triboelectric MXene-based 3D printed wearable sensor for real-time health monitoring.<sup>173</sup> This device exhibited excellent performance. For example, the power output is  $816.6 \text{ mW m}^{-2}$ , the sensitivity reaches  $6.03 \text{ kPa}^{-1}$ , the low detection limit is 9 Pa and the fast response time is only 80 ms. Yu *et al.* reported a triboelectric tactile sensor using ultra-stretchable and conductive hydrogels based on carbon. The sensitivity of this device reached a gauge factor of 2.6, and the broad strain response range is 0–2000%.<sup>174</sup> Additionally, the hydrogel can be fabricated as a flexible self-powered triboelectric electrode, the detecting pressure range is 1–25 N, and the short-circuit current is  $2.6 \mu\text{A}$ .

### 6.2 Cardiovascular monitoring

It is well known that cardiovascular disease is a leading cause of mortality worldwide. Therefore, the development of wearable electronics for cardiovascular disease monitoring has great value. Arterial pulse waves can give comprehensive cardiovascular information for diagnosing disease. Fang *et al.* reported a machine-learning assisted textile triboelectric micro-pressure sensor for cardiovascular monitoring. This triboelectric pressure sensor holds a response time of 40 ms and a sensitivity of  $0.21 \mu\text{A kPa}^{-1}$ .<sup>175</sup> Lou *et al.* developed a triboelectric sensing textile constructed with core–shell yarns to detect the pulse monitoring. The sensitivity of this sensor is  $1.33 \text{ V kPa}^{-1}$  and



Table 2 The pressure measurement ranges of the triboelectric pressure sensors

Materials	Sensitivity	Detection range	Detection limit
Mxene <sup>173</sup>	6.03 kPa <sup>-1</sup>	Not known	9 Pa
Ag nanowires <sup>180</sup>	0.1 nA kPa <sup>-1</sup>	Not known	Not known
CNTs <sup>175</sup>	0.21 μA kPa <sup>-1</sup>	Not known	Not known
P(VDF-TrFE) <sup>181</sup>	2.2 V kPa <sup>-1</sup>	0.1–98 kPa	Not known
PDMS <sup>182</sup>	3.627 kPa <sup>-1</sup>	0–8 kPa	5 Pa
	1.264 kPa <sup>-1</sup>	8–80 kPa	5 Pa
Porous PDMS <sup>183</sup>	54.37 mV kPa <sup>-1</sup>	0–80 kPa	Not known
	9.80 mV kPa <sup>-1</sup>	80–240 kPa	Not known
PDMS <sup>184</sup>	249.32 mV kPa <sup>-1</sup>	0–450 kPa	8.72 Pa
PDMS/Ag <sup>185</sup>	1.67 V kPa <sup>-1</sup>	0–3 kPa	Not known
	0.20 V kPa <sup>-1</sup>	3–32 kPa	Not known
PTFE-Nylon <sup>176</sup>	1.33 V kPa <sup>-1</sup>	1.95–3.13 kPa	Not known
	0.32 V kPa <sup>-1</sup>	3.20–4.61 kPa	Not known
TATSA <sup>177</sup>	7.84 mV Pa <sup>-1</sup>	Not known	Not known
Hydrogel <sup>174</sup>	GF = 2.6	1–25 N	Not known
Chitosan@starch-FEP <sup>179</sup>	46.03 V kPa <sup>-1</sup>	1.25–6.25 kPa	Not known

0.32 V kPa<sup>-1</sup> in the pressure ranges of 1.95–3.13 kPa and 3.20–4.61 kPa, respectively.<sup>176</sup> More importantly, the triboelectric sensing textile can capture real-time pulse signals and reflect the current health status.

Considering that most reported wearable textile sensors can only monitor a single physiological signal, some researchers have reported on a triboelectric textile sensor array to monitor the arterial pulse waves and respiratory signals simultaneously.<sup>177</sup> The measuring results of the triboelectric textile sensor array showed that its pressure sensitivity, fast response time, stability and wide working frequency bandwidth are

7.84 mV Pa<sup>-1</sup>, 20 ms, 100 000 cycles and 20 Hz, respectively. This device realized a long-term and non-invasive health monitoring of cardiovascular disease and sleep apnea syndrome.

### 6.3 Motion monitoring

Flexible, wearable and self-powered pressure sensors for motion detection are attracting wide attention due to its saving energy. Some researchers are developing self-powered pressure sensors based on the triboelectric effect for motion monitoring. Kim *et al.* reported a pressure sensor based on triboelectric-

Table 3 Performances of the flexible pressure sensors

Mechanism	Materials	Sensitivity	Detection range	Detection limit	Response time
Triboelectric	Mxene <sup>173</sup>	6.03 kPa <sup>-1</sup>	Not known	9 Pa	80 ms
	Ag nanowires <sup>180</sup>	0.1 nA kPa <sup>-1</sup>	Not known	Not known	0.2 s
	P(VDF-TrFE) <sup>181</sup>	2.2 V kPa <sup>-1</sup>	0.1–98 kPa	Not known	Not known
	PDMS <sup>182</sup>	3.627 kPa <sup>-1</sup>	0–8 kPa	5 Pa	40 ms
		1.264 kPa <sup>-1</sup>	8–80 kPa	5 Pa	5 Pa
	Porous PDMS <sup>183</sup>	54.37 mV kPa <sup>-1</sup>	0–80 kPa	Not known	Not known
		9.80 mV kPa <sup>-1</sup>	80–240 kPa	Not known	Not known
	PDMS <sup>184</sup>	249.32 mV kPa <sup>-1</sup>	0–450 kPa	8.72 Pa	26 ms
	PDMS/Ag <sup>185</sup>	1.67 V kPa <sup>-1</sup>	0–3 kPa	Not known	Not known
		0.20 V kPa <sup>-1</sup>	3–32 kPa	Not known	Not known
Capacitive	PS/Au/PDMS <sup>186</sup>	0.0047 kPa <sup>-1</sup>	0–50 N	17.5 Pa	38 ms
	AgNWs/PDMS <sup>187</sup>	1.2 kPa <sup>-1</sup>	50–500 N	17.5 Pa	38 ms
		0.08 kPa <sup>-1</sup>	0–2 kPa	0.8 Pa	36 ms
	Au/PDMS <sup>188</sup>	0.6 kPa <sup>-1</sup>	2–14.5 kPa	0.8 Pa	58 ms
	PDMS <sup>189</sup>	0.55 kPa <sup>-1</sup>	0–1 kPa	4.5 Pa	180 ms
Piezoelectric	Liquid metal <sup>190</sup>	1.1 kPa <sup>-1</sup>	Not known	3 Pa	Not known
	OTFT <sup>191</sup>	8.4 kPa <sup>-1</sup>	0–60 kPa	4 Pa	<60 ms
	P(VDF-TrFe) <sup>192</sup>	1.1 kPa <sup>-1</sup>	0–1–2 kPa	Not known	10 ms
	2D ZnO <sup>193</sup>	60.97–78.23 meV MPa <sup>-1</sup>	0–3.64 MPa	Not known	Not known
Piezoresistive	ZnO <sup>194</sup>	1448.08–1677.53 meV MPa <sup>-1</sup>	0–152.88 kPa	Not known	5 ms
	SWNTs <sup>195</sup>	2.2 kPa <sup>-1</sup>	35–2500 Pa	Not known	5 ms
		1.3 kPa <sup>-1</sup>	2500–11700 Pa	Not known	Not known
	PDMS <sup>196</sup>	0.23 kPa <sup>-1</sup>	<10 kPa	1 Pa	Not known
	GO <sup>197</sup>	17.2 kPa <sup>-1</sup>	0–20 kPa	Not known	Not known
	Graphene textile <sup>198</sup>	0.012 kPa <sup>-1</sup>	<800 kPa	Not known	50 ms



flexoelectric nanogenerators for human motion monitoring, such as eye blinking, finger bending, knee bending and swallowing.<sup>178</sup> Because the device combines the triboelectric–flexoelectric effect, it shows a higher sensitivity of up to 0.173 V kPa<sup>-1</sup>. Zheng *et al.* designed a transparent triboelectric nanogenerator for monitoring human motion exhibits ultrahigh sensitivity and is eco-friendly. This TENG consisted of a chitosan@starch composite film with the fluorinated ethylene propylene film and transparent PET/ITO electrodes, and its sensitivity reached to 46.03 V kPa<sup>-1</sup> in the pressure range of 1.25–6.25 kPa.<sup>179</sup>

The range of pressure measurement is one of the most crucial parameters for triboelectric pressure sensors. Table 2 shows the pressure measurement ranges of reported triboelectric pressure sensors. The pressure measurement ranges of most triboelectric pressure sensors are narrow. Therefore, it is a great challenge to improve the pressure measurement range. Xu *et al.* proposed a wide-range triboelectric pressure sensor based on the different Young's modulus values of materials and a double-sandwich-structure design. This device has an excellent range of pressure measurement of 0–450 kPa.<sup>184</sup> Meanwhile, the other performance parameters also are superior; for example, the sensitivity is 249.32 mV kPa<sup>-1</sup>, the response time is 26 ms, and the detection limit is 8.72 Pa. Thus, this triboelectric pressure sensor can be used to detect small motion, and it can combine a convolutional gated recurrent unit model to recognize four human motions with 99.42% accuracy.

## 7 Conclusions

Wearable health monitoring devices have attracted significant attention from medical and scientific researchers because it is able to monitor the body status in real-time. In this review, the recent progress on flexible micro-pressure sensors for wearable health monitoring is presented. In view of the current popular topics of health monitoring, such as heart, blood pressure and body motions, we have summarized and discussed in detail the applications of flexible micro-pressure sensors with four types of sensing mechanism (piezoresistive, capacitive, piezoelectric and triboelectric) in these research fields. The performances of these four type pressure sensors are shown in Table 3. Finally, the challenges and perspectives in flexible micro-pressure sensors for wearable health monitoring are discussed as follows.

### 7.1 Future challenges

Developing flexible micro-pressure sensors with high performance for wearable health monitoring are still a great challenge. First, the stretchability of flexible micro-pressure sensors still needs to be improved because it should bond to non-planar human skin. Flexible micro-pressure sensors also need large bending characteristics. Second, the pressure detection range of most of the existing flexible micro-pressure sensors is relatively narrow, so it is necessary to develop flexible sensors with a wide pressure detection range. Third, the sensitivity of the flexible micro-pressure sensor needs to be improved. In the process of micro-pressure detection, because the required signal is very small, other signals often drown out the pressure signal to be detected,

resulting in not being able to detect the signal they need. Namely, we need to improve the sensitivity of the sensor. In general, these challenges can be solved by developing materials with high performance and designing novel sensor structures. Moreover, reducing production costs and achieving mass production of flexible micro-pressure sensors remain a huge challenge.

### 7.2 Outlook

With the emphasis on climate and environmental protection and the limitation of carbon emissions, wearable flexible pressure sensors will develop in the direction of ultra-sensitivity, environment-friendliness, biocompatibility and self-energy supply in the future. First, the development of flexible micro-pressure sensors with ultra-sensitivity is an important trend. Ultra-sensitivity is a basic requirement to perform the monitoring of weak physiological signals. Moreover, it also can improve the resolution of the sensor. Second, it is necessary to develop flexible micro-pressure sensors with excellent biocompatibility. Excellent biocompatibility will ensure that the sensor will not cause harm to the human body, which allows it to be worn for a long time to monitor the body's physiological signals. Third, a wearable flexible micro-pressure sensor that can realize self-energy supply has an important prospect. Self-powered sensors ensure that they do not need to be worn and unloaded frequently for charging operation, which can greatly save energy and significantly improve the service during their lifespan. Fourth, one-dimensional (1D) and two-dimensional (2D) nanomaterials will bring great changes to the flexible pressure sensors due to their excellent advantages, such as light-weight property, flexibility, durability, large surface area, excellent electrical conductivity, and high mechanical strength. Finally, combined with artificial intelligence and other technologies, it is very meaningful to develop flexible micro-pressure sensors to meet personalized medical needs. Due to the different physical qualities of each person, it is a realistic need to combine artificial intelligence and other technologies to achieve personalized health monitoring. This can then achieve an accurate physical condition analysis for each individual body, thus providing great help for better medical diagnosis.

## Conflicts of interest

There are no conflicts to declare.

## Acknowledgements

This work is supported by the National Key R&D Program (2021YFC3002200, 2020YFA0709800, 2018YFC2001202), the National Natural Science Foundation of China (U20A20168, 61874065, 51861145202), and the China Postdoctoral Science Foundation (No. 2022M721896).

## References

- 1 S. Kim, M. Amjadi, T. I. Lee, Y. Jeong, D. Kwon, M. S. Kim, K. Kim, T. S. Kim, Y. S. Oh and I. Park, *ACS Appl. Mater. Interfaces*, 2019, **11**, 23639.



2 X. Xiao, X. Xiao, Y. Zhou, X. Zhao, G. Chen, Z. Liu, Z. Wang, C. Lu, M. Hu, A. Nashalian, S. Shen, K. Xie, W. Yang, Y. Gong, W. Ding, P. Servati, C. Han, S. Dou, W. Li and J. Chen, *Sci. Adv.*, 2021, **7**, eabl3742.

3 Y. An, Y. Ren, M. Bick, A. Dudek, E. H.-W. Waworuntu, J. Tang, J. Chen and B. Chang, *Biosens. Bioelectron.*, 2020, **154**, 112078.

4 Y. Su, T. Yang, X. Zhao, Z. Cai, G. Chen, M. Yao, K. Chen, M. Bick, J. Wang, S. Li, G. Xie, H. Tai, X. Du, Y. Jiang and J. Chen, *Nano Energy*, 2020, **74**, 104941.

5 T. Tat, A. Libanori, C. Au, A. Yau and J. Chen, *Biosens. Bioelectron.*, 2021, **171**, 112714.

6 Y. Su, J. Wang, B. Wang, T. Yang, B. Yang, G. Xie, Y. Zhou, S. Zhang, H. Tai, Z. Cai, G. Chen, Y. Jiang, L.-Q. Chen and J. Chen, *ACS Nano*, 2020, **14**, 6067.

7 X. Xiao, X. Xiao, A. Nashalian, A. Libanori, Y. Fang, X. Li and J. Chen, *Adv. Healthcare Mater.*, 2021, **10**, 2100975.

8 B. C. K. Tee, A. Chortos, R. R. Dunn, G. Schwartz, E. Eason and Z. A. Bao, *Adv. Funct. Mater.*, 2014, **24**, 5427.

9 Y. Wei, S. Chen, Y. Lin, Z. M. Yang and L. Liu, *J. Mater. Chem. C*, 2015, **3**, 9594–9602.

10 F. Liu, F. Han, L. Ling, J. Li, S. Zhao, T. Zhao, X. Liang, D. Zhu, G. Zhang, R. Sun, D. Ho and C. P. Wong, *Chemistry*, 2018, **24**, 16823.

11 M. Ha, S. Lim, S. Cho, Y. Lee, S. Na, C. Baig and H. Ko, *ACS Nano*, 2018, **12**, 3964.

12 P. Wei, X. Guo, X. Qiu and D. Yu, *Nanotechnology*, 2019, **30**, 455501.

13 F.-R. Fan, L. Lin, G. Zhu, W. Wu, R. Zhang and Z. L. Wang, *Nano Lett.*, 2012, **12**, 3109.

14 Q. J. Sun, J. Zhuang, S. Venkatesh, Y. Zhou, S. T. Han, W. Wu, K.-W. Kong, W. J. Li, X. Chen, R. K. Y. Li and V. A. L. Roy, *ACS Appl. Mater. Interfaces*, 2018, **10**, 4086.

15 C. Pang, G. Y. Lee, T. I. Kim, S. M. Kim, H. N. Kim, S. H. Ahn and K. Y. Suh, *Nat. Mater.*, 2012, **11**, 795.

16 X. F. Zhao, C. Z. Hang, X. H. Wen, M. Y. Liu, H. Zhang, F. Yang, R. G. Ma, J. C. Wang, D. W. Zhang and H. L. Lu, *ACS Appl. Mater. Interfaces*, 2020, **12**, 14136.

17 G. Schwartz, B. C. K. Tee, J. Mei, A. L. Appleton, D. H. Kim, H. Wang and Z. Bao, *Nat. Commun.*, 2013, **4**, 1859.

18 Y. Gao, C. Lu, Y. Guohui, J. Sha, J. Tan and F. Xuan, *Nanotechnology*, 2019, **30**, 325502.

19 S. R. A. Ruth, L. Beker, H. Tran, V. R. Feig, N. Matsuhisa and Z. Bao, *Adv. Funct. Mater.*, 2019, **30**, 1903100.

20 T. Zhao, L. Yuan, T. Li, L. Chen, X. Li and J. Zhang, *ACS Appl. Mater. Interfaces*, 2020, **12**, 55362.

21 K. Y. Meng, X. Xiao, W. X. Wei, G. R. Chen, A. Nashalian, S. Shen, X. Xiao and J. Chen, *Adv. Mater.*, 2022, **34**, 2109357.

22 W. Gao, S. Emaminejad, H. Y. Nyein, S. Challa, K. Chen, A. Peck, H. M. Fahad, H. Ota, H. Shiraki, D. Kiriya, D. H. Lien, G. A. Brooks, R. W. Davis and A. Javey, *Nature*, 2016, **529**, 509.

23 I. Korhonen, J. Parkka and M. V. Gils, *IEEE Eng. Med. Biol. Mag.*, 2003, **22**, 66.

24 C. Dagdeviren, Y. Su, P. Joe, R. Yona, Y. Liu, Y. S. Kim, Y. Huang, A. R. Damadoran, J. Xia, L. W. Martin, Y. Huang and J. A. Rogers, *Nat. Commun.*, 2014, **5**, 4496.

25 G. Schwartz, B. C. Tee, J. Mei, A. L. Appleton, H. Kim do, H. Wang and Z. Bao, *Nat. Commun.*, 2013, **4**, 1859.

26 L. Guan, A. Nilghaz, B. Su, L. Jiang, W. Cheng and W. Shen, *Adv. Funct. Mater.*, 2016, **26**, 4511.

27 S. Gong, D. T. H. Lai, B. Su, K. J. Si, Z. Ma, L. W. Yap, P. Guo and W. Chen, *Adv. Electron. Mater.*, 2015, **1**, 1400063.

28 A. Vorobyov and C. Henemann, Dallemande, in *10th European Conference on Antennas and Propagation (EuCAP)*, IEEE, Davos, Switzerland, 2016, vol. 1.

29 A. Plichta, A. Weber and A. Habeck, in *MRS Proceedings*, 2003, 769; Z. Ma, B. Su, S. Gong, Y. Wang, L. W. Yap, G. P. Simon and W. Cheng, *ACS Sens.*, 2016, **1**, 303.

30 Y. Wang, S. Gong, S. Wang, G. P. Simon and W. Cheng, *Mater. Horiz.*, 2016, **3**, 208.

31 C. Sheridan, *Nat. Biotechnol.*, 2014, **32**, 965.

32 X. Wang, Y. Gu, Z. Xiong, Z. Cui and T. Zhang, *Adv. Mater.*, 2014, **26**, 1336.

33 D. H. Kim, N. Lu, R. Ma, Y. S. Kim, R. H. Kim, S. Wang, J. Wu, S. M. Won, H. Tao, A. Islam, K. J. Yu, T. I. Kim, R. Chowdhury, M. Ying, L. Xu, M. Li, H. J. Chung, H. Keum, M. McCormick, P. Liu, Y. W. Zhang, F. G. Omenetto, Y. Huang, T. Coleman and J. A. Rogers, *Science*, 2011, **333**, 838.

34 X. Liu, J. Liu, J. Wang, T. Wang, Y. Jiang, J. Hu, Z. Liu, X. Chen and J. Yu, *ACS Appl. Mater. Interfaces*, 2020, **12**, 5601.

35 Y. Pang, K. Zhang, Z. Yang, S. Jiang, Z. Ju, Y. Li, X. Wang, D. Wang, M. Jian, Y. Zhang, R. Liang, H. Tian, Y. Yang and T. L. Ren, *ACS Nano*, 2018, **12**, 2346.

36 T. Zhao, T. Li, L. Chen, L. Yuan, X. Li and J. Zhang, *ACS Appl. Mater. Interfaces*, 2019, **11**, 29466.

37 M. Ezzati, Z. Obermeyer, I. Tzoulaki, B. M. Mayosi, P. Elliott and D. A. Leon, *Nat. Rev. Cardiol.*, 2015, **12**, 508.

38 S. Chen, J. Qi, S. Fan, Z. Qiao, J. C. Yeo and C. T. Lim, *Adv. Healthcare Mater.*, 2021, **10**, 2100116.

39 M. Houston, *Ther. Adv. Cardiovasc. Dis.*, 2018, **12**, 85.

40 M. H. Olsen, S. Y. Angell, S. Asma, P. Boutouyrie, D. Burger, J. A. Chirinos, A. Damasceno, C. Delles, A. P. Gimenez-Roqueplo, D. Hering, P. Lopez-Jaramillo, F. Martinez, V. Perkovic, E. R. Rietzschel, G. Schillaci, A. E. Schutte, A. Scuteri, J. E. Sharman, K. Wachtell and J. G. Wang, *Lancet*, 2016, **388**, 2665.

41 D. Ettehad, C. A. Emdin, A. Kiran, S. G. Anderson, T. Callender, J. Emberson, J. Chalmers, A. Rodgers and K. Rahimi, *Lancet*, 2016, **387**, 957.

42 B. Zhou, G. Danaei, G. A. Stevens, H. Bixby, C. Taddei, R. M. Carrillo-Larco, B. Solomon, L. M. Riley, M. Di Cesare, M. L. C. Iurilli, A. Rodriguez-Martinez, A. Zhu, K. Hajifathalian, A. Amuzu, J. R. Banegas, J. E. Bennett, C. Cameron, Y. Cho, J. Clarke, C. L. Craig, J. J. Cruz, L. Gates, S. Giampaoli, E. W. Gregg, R. Hardy, A. J. Hayes, N. Ikeda, R. T. Jackson, G. Jennings, M. Joffres, *et al.*, *Lancet*, 2019, **394**, 639.

43 K. Jin, S. Khonsari, R. Gallagher, P. Gallagher, A. M. Clark, B. Freedman, T. Briffa, A. Bauman, J. Redfern and L. Neubeck, *Eur. J. Cardiovasc. Nurs.*, 2019, **18**, 260.



44 R. J. McManus, J. Mant, M. Franssen, A. Nickless, C. Schwartz, J. Hodgkinson, P. Bradburn, A. Farmer, S. Grant, S. M. Greenfield, C. Heneghan, S. Jowett, U. Martin, S. Milner, M. Monahan, S. Mort, E. Ogburn, R. Perera-Salazar, S. A. Shah, L. M. Yu, L. Tarassenko, F. D. R. Hobbs and T. Investigators, *Lancet*, 2018, **391**, 949.

45 X. Xiao, G. Chen, A. Libanori and J. Chen, *Trends Chem.*, 2021, **3**, 279.

46 S. Shen, X. Xiao, X. Xiao and J. Chen, *Chem. Commun.*, 2021, **57**, 5871.

47 S. Zhang, M. Bick, X. Xiao, G. Chen and A. Nashalian, *J. Mater. Chem.*, 2021, **4**, 845.

48 S. W. Chen, N. Wu, S. Z. Lin, J. J. Duan, Z. S. Xu, Y. Pan, H. B. Zhang, Z. H. Xu, L. Huang, B. Hu and J. Zhou, *Nano Energy*, 2020, **70**, 104460.

49 Y. X. Xiong, Y. K. Shen, L. Tian, Y. G. Hu, P. L. Zhu, R. Sun and C. P. Wong, *Nano Energy*, 2020, **70**, 104436.

50 J. He, P. Xiao, W. Lu, J. W. Shi, L. Zhang, Y. Liang, C. F. Pan, S. W. Kuo and T. Chen, *Nano Energy*, 2019, **59**, 422–433.

51 Y. Guo, M. J. Zhong, Z. W. Fang, P. B. Wan and G. H. Yu, *Nano Lett.*, 2019, **19**, 1143–1150.

52 Y. Y. Gao, C. Yan, H. C. Huang, T. Yang, G. Tian, D. Xiong, N. J. Chen, X. Chu, S. Zhong, W. L. Deng, Y. Fang and W. Q. Yang, *Adv. Funct. Mater.*, 2020, **30**, 1909603.

53 G. Li, D. Chen, C. L. Li, W. X. Liu and H. Liu, *Adv. Sci.*, 2020, **7**, 2000154.

54 L. X. Mo, X. Y. Meng, J. Zhao, Y. Q. Pan, Z. C. Sun, Z. X. Guo, W. Wang, Z. C. Peng, C. Shang, S. B. Han, K. Hu, M. J. Cao, Y. J. Chen, Z. Q. Xin, J. S. Lu and L. H. Li, *Flexible Printed Electron.*, 2021, **6**, 014001.

55 Z. Lou, S. Chen, L. L. Wang, R. L. Shi, L. Li, K. Jiang, D. Chen and G. Z. Shen, *Nano Energy*, 2017, **38**, 28–35.

56 M. J. Zhong, L. J. Zhang, X. Liu, Y. N. Zhou, M. Y. Zhang, Y. J. Wang, L. Yang and D. Wei, *Chem. Eng. J.*, 2021, **412**, 128649.

57 L. Zhang, K. S. Kumar, H. He, C. J. Cai, X. He, H. Gao, S. Yue, C. Li, R. C. Seet, H. Ren and J. Ouyang, *Nat. Commun.*, 2020, **11**, 4683.

58 I. You, D. G. Mackanic, N. Matsuhisa, J. Kang, J. Kwon, L. Beker, J. Mun, W. Suh, T. Y. Kim, J. B. Tok, Z. Bao and U. Jeong, *Science*, 2020, **370**, 961.

59 A. L. Pauca, M. F. O'Rourke and N. D. Kon, *Hypertension*, 2001, **38**, 932.

60 Y. Fang, X. Zhao, T. Tat, X. Xiao, G. Chen and J. Xu, *J. Mater. Chem.*, 2021, **4**, 1102.

61 J. Park, J. Kim, K. Kim, S. Y. Kim, W. H. Cheong, K. Park, J. H. Song, G. Namgoong, J. J. Kim, J. Heo, F. Bien and J. U. Park, *Nanoscale*, 2016, **8**, 10591–10597.

62 T. Q. Trung, L. T. Duy, S. Ramasundaram and N.-E. Lee, *Nano Res.*, 2017, **10**, 2021–2033.

63 D. Kim, D. Kim, H. Lee, Y. R. Jeong, S. J. Lee, G. Yang, H. Kim, G. Lee, S. Jeon, G. Zi, J. Kim and J. S. Ha, *Adv. Mater.*, 2016, **28**, 748–756.

64 W. Yang, N.-W. Li, S. Zhao, Z. Yuan, J. Wang, X. Du, B. Wang, R. Cao, X. Li, W. Xu, Z. L. Wang and C. Li, *Adv. Mater. Technol.*, 2018, **3**, 1700241.

65 L. Q. Tao, K. N. Zhang, H. Tian, Y. Liu, D. Y. Wang, nY. Q. Chen, Y. Yang and T. L. Ren, *ACS Nano*, 2017, **11**, 8790–8795.

66 S. Gong, W. Schwalb, Y. Wang, Y. Chen, Y. Tang, J. Si, B. Shirinzadeh and W. Cheng, *Nat. Commun.*, 2014, **5**, 3132.

67 E. M. G. Rodrigues, R. Godina, C. M. P. Cabrita and J. P. S. Catalao, *Biomed. Signal Process. Control*, 2017, **31**, 419.

68 Z. Zhou, K. Chen, X. Li, S. Zhang, Y. Wu, Y. Zhou, K. Meng, C. Sun, Q. He, W. Fan, E. D. Fan, Z. Lin, X. Tan, W. Deng, J. Yang and J. Chen, *Nat. Electron.*, 2020, **3**, 571.

69 W. Fan, Q. He, K. Meng, X. Tan, Z. Zhou, G. Zhang, J. Yang and Z. L. Wang, *Sci. Adv.*, 2020, **6**, 2840.

70 X. C. Dong, Y. Wei, S. Chen, Y. Lin, L. Liu and J. Li, *Compos. Sci. Technol.*, 2018, **155**, 108–116.

71 Z. L. Huang, M. Gao, Z. C. Yan, T. S. Pan, S. A. Khan, Y. Zhang, H. L. Zhang and Y. Lin, *Sens. Actuators, A*, 2017, **266**, 345–351.

72 Z. Y. Yue, X. K. Ye, S. H. Liu, Y. C. Zhu, H. D. Jiang, Z. Q. Wan, Y. Lin and C. Y. Jia, *Biosens. Bioelectron.*, 2019, **139**, 111296.

73 H. R. Kou, L. Zhang, Q. L. Tan, G. Y. Liu, W. Lv, F. X. Lu, H. L. Dong and J. J. Xiong, *Sens. Actuators, A*, 2018, **277**, 150–156.

74 M. D. Xu, Y. Gao, G. H. Yu, C. Lu, J. P. Tan and F. Z. Xuan, *Sens. Actuators, A*, 2018, **284**, 260–265.

75 Y. Gao, G. H. Yu, J. P. Tan and F. Z. Xuan, *Sens. Actuators, A*, 2018, **280**, 205–209.

76 W. Li, X. Jin, Y. D. Zheng, X. D. Chang, W. Y. Wang, T. Lin, F. Zheng, O. Onyilagha and Z. T. Zhu, *J. Mater. Chem. C*, 2020, **8**, 11468.

77 Y. B. Wan, Z. G. Qiu, Y. Hong, Y. Wang, J. M. Zhang, Q. X. Liu, Z. G. Wu and C. F. Guo, *Adv. Electron. Mater.*, 2018, **4**, 1700586.

78 Y. Adesida, E. Papi and A. H. McGregor, *Sensors*, 2019, **19**, 1597.

79 M. Munoz-Organero, J. Parker, L. Powell and S. Mawson, *Sensors*, 2016, **16**, 1631.

80 P. Porciuncula, A. V. Roto, D. Kumar, I. Davis, S. Roy, C. J. Walsh and L. N. Awad, *PM&R*, 2018, **10**, S220–S232.

81 W. Gao, H. Ota, D. Kiriya, K. Takei and A. Javey, *Acc. Chem. Res.*, 2019, **52**, 523.

82 T. Someya and M. Amagai, *Nat. Biotechnol.*, 2019, **37**, 382.

83 T. R. Ray, J. Choi, A. J. Bandodkar, S. Krishnan, P. Gutruf, L. Tian, R. Ghaffari and J. A. Rogers, *Chem. Rev.*, 2019, **119**, 5461.

84 S. Chen, L. J. Sun, X. J. Zhou, Y. F. Guo, J. C. Song, S. H. Qian, Z. H. Liu, Q. B. Guan, E. M. Jeffries, W. G. Liu, Y. D. Wang, C. L. He and Z. W. You, *Nat. Commun.*, 2020, **11**, 1107.

85 S. Gong and W. Cheng, *Adv. Electron. Mater.*, 2017, **3**, 1600314.

86 S. Yao, P. Swetha and Y. Zhu, *Adv. Healthcare Mater.*, 2018, **7**, 1700889.

87 X. Wang, Z. Liu and T. Zhang, *Small*, 2017, **13**, 1602790.

88 Y. Liu, M. Pharr and G. A. Salvatore, *ACS Nano*, 2017, **11**, 9614–9635.



89 J. Heikenfeld, A. Jajack, J. Rogers, P. Gutruf, L. Tian, T. Pan, R. Li, M. Khine, J. Kim, J. Wang and J. Kim, *Lab Chip*, 2018, **18**, 217–248.

90 Z. Ma, S. Li, H. Wang, W. Cheng, Y. Li, L. Pan and Y. Shi, *J. Mater. Chem. B*, 2019, **7**, 173–197.

91 Y. L. Wang, Y. N. Yu, X. Y. Wei and F. Narita, *Adv. Mater. Technol.*, 2022, 2200318.

92 R. J. Sun, S. C. Carreira, Y. Chen, C. Q. Xiang, L. L. Xu, B. Zhang, M. D. Chen, I. Farrow, F. Scarpa and J. Rossiter, *Adv. Mater. Technol.*, 2019, **4**, 1900100.

93 J. Park, Y. Lee, J. Hong, M. Ha, Y. D. Jung, H. Lim, S. Y. Kim and H. Ko, *ACS Nano*, 2014, **8**, 4689.

94 M. Jian, K. Xia, Q. Wang, Z. Yin, H. Wang, C. Wang, H. Xie, M. Zhang and Y. Zhang, *Adv. Funct. Mater.*, 2017, **27**, 1606066.

95 Y. D. Li, Y. N. Li, M. Su, W. B. Li, Y. F. Li, H. Z. Li, X. Qian, X. Y. Zhang, F. Y. Li and Y. L. Song, *Adv. Electron. Mater.*, 2017, **3**, 1700253.

96 D. J. Lipomi, M. Vosgueritchian, B. C. K. Tee, S. L. Hellstrom, J. A. Lee, C. H. Fox and Z. Bao, *Nat. Nanotechnol.*, 2011, **6**, 788.

97 T. Li, H. Luo, L. Qin, X. Wang, Z. Xiong, H. Ding, Y. Gu, Z. Liu and T. Zhang, *Small*, 2016, **12**, 5042.

98 S. H. Cho, S. W. Lee, S. Yu, H. Kim, S. Chang, D. Kang, I. Hwang, H. S. Kang, B. Jeong, E. H. Kim, S. M. Cho, K. L. Kim, H. Lee, W. Shim and C. Park, *ACS Appl. Mater. Interfaces*, 2017, **9**, 10128.

99 S. Kang, J. Lee, S. Lee, S. Kim, J.-K. Kim, H. Algadi, S. Al-Sayari, D.-E. Kim, D. Kim and T. Lee, *Adv. Electron. Mater.*, 2016, **2**, 1600356.

100 W. Wu, X. Wen and Z. L. Wang, *Science*, 2013, **340**, 952.

101 Z. F. Chen, Z. Wang, X. M. Li, Y. X. Lin, N. Q. Luo, M. Z. Long, N. Zhao and J. B. Xu, *ACS Nano*, 2017, **11**, 4507.

102 F. R. Fan, L. Lin, G. Zhu, W. Wu, R. Zhang and Z. L. Wang, *Nano Lett.*, 2012, **12**, 3109.

103 T. Li, J. Zou, F. Xing, M. Zhang, X. Cao, N. Wang and Z. L. Wang, *ACS Nano*, 2017, **11**, 3950.

104 M. Cao, J. Su, S. Fan, H. Qiu, D. Su and L. Li, *Chem. Eng. J.*, 2021, **406**, 126777.

105 N. Luo, W. Dai, C. Li, Z. Zhou, L. Lu, C. C. Y. Poon, S.-C. Chen, Y. Zhang and N. Zhao, *Adv. Funct. Mater.*, 2016, **26**, 1178–1187.

106 Y. Q. Liu, Y. L. Zhang, Z. Z. Jiao, D. D. Han and H. B. Sun, *Nanoscale*, 2018, **10**, 17002–17006.

107 N. Yu Dhanjai and S. M. Mugo, *Talanta*, 2019, **204**, 602–606.

108 M. V. Antipov, I. V. Yurtov, A. A. Utenkov, A. V. Fedoseev, V. A. Ogorodnikov and A. L. Mikhailov, *J. Exp. Theor. Phys.*, 2020, **130**, 517–522.

109 E. S. Hosseini, L. Manjakkal, D. Shakthivel and R. Dahiya, *ACS Appl. Mater. Interfaces*, 2020, **12**, 9008–9016.

110 M. Zhu, S. S. Chng, W. Cai, C. Liu and Z. Du, *RSC Adv.*, 2020, **10**, 21887–21894.

111 L. Lin, Y. N. Xie, S. H. Wang, W. Z. Wu, S. Niu, X. N. Wen and Z. L. Wang, *ASC Nano*, 2013, **7**, 8266.

112 G. Laszlo, E. M. Nicholson, J. Denison and P. R. Goddard, *Lancet*, 2000, **356**, 737.

113 Y. Pang, H. Tian, L. Tao, Y. Li, X. Wang, N. Deng, Y. Yang and T. L. Ren, *ACS Appl. Mater. Interfaces*, 2016, **8**, 26458.

114 Z. Xiaoli, H. Qilin, Y. Ruomeng, Z. Yan and P. Caofeng, *Adv. Electron. Mater.*, 2015, **1**, 1500142.

115 S. C. Mannsfeld, B. C. Tee, R. M. Stoltzberg, C. V. Chen, n S. Barman, B. V. Muir, A. N. Sokolov, C. Reese and Z. Bao, *Nat. Mater.*, 2010, **9**, 859–864.

116 B. C. K. Tee, A. Chortos, R. R. Dunn, G. Schwartz, E. Eason and Z. A. Bao, *Adv. Funct. Mater.*, 2014, **24**, 5427–5434.

117 K. Hyehohn, K. Gwangmook, K. Taehoon, L. Sangwoo, K. Donyoung, H. Min-Soo, C. Youngcheol, K. Shinill, L. Hyungsuk, P. Hong-Gyu and S. Wooyoung, *Small*, 2018, **14**, 1703432.

118 C. Wan and C. R. Bowen, *J. Mater. Chem. A*, 2017, **5**, 3091–3128.

119 C. Deng, W. Tang, L. Liu, B. Chen, M. Li and Z. L. Wang, *Adv. Funct. Mater.*, 2018, **28**, 1–9.

120 K. S. Ramadan, D. Sameoto and S. Evoy, *Smart Mater. Struct.*, 2014, **23**, 033001.

121 F. R. Fan, Z. Q. Tian and Z. L. Wang, *Nano Energy*, 2012, **1**, 328–334.

122 W. Xu, H. Zheng, Y. Liu, X. Zhou, C. Zhang, Y. Song, X. Deng, M. Leung, Z. Yang, R. X. Xu, Z. L. Wang, X. C. Zeng and Z. Wang, *Nature*, 2020, **578**, 392–396.

123 R. Hinchet, H. J. Yoon, H. Ryu, M. K. Kim, E. K. Choi, D. S. Kim and S. W. Kim, *Science*, 2019, **365**, 491–494.

124 F. R. Fan, L. Lin, G. Zhu, W. Wu, R. Zhang and Z. L. Wang, *Nano Lett.*, 2012, **12**, 3109–3114.

125 M. G. Wang, J. J. Wu, L. Dong, J. Shi, Q. Gao, C. H. Zhu and H. Morikawa, *J. Mater. Chem. C*, 2022, **10**, 12323.

126 H. N. Cheng, Y. S. Tan, N. Y. Zhang, Y. J. Yin and C. X. Wang, *Adv. Mater. Interfaces*, 2022, **9**, 2200614.

127 L. Pu, Y. Liu, L. Li, C. Zhang, P. Ma, W. Dong, Y. Huang and T. Liu, *ACS Appl. Mater. Interfaces*, 2021, **13**, 47134.

128 D. P. Hao, R. X. Yang, N. Yi and H. Y. Cheng, *Sci. China: Technol. Sci.*, 2021, **64**, 2408–2414.

129 L. Q. Yuan, Z. W. Wang, H. W. Li, Y. N. Huang, S. G. Wang, X. Gong, Z. T. Tan, Y. X. Hu, X. S. Chen, J. Li, H. Z. Lin, L. Q. Li and W. P. Hu, *Adv. Mater. Technol.*, 2020, **5**, 1901084.

130 Y. W. Zhao, X. Li, T. Yuan, S. H. Huang, R. H. Jiang, X. F. Duan, L. Li, X. T. Li and W. M. Zhang, *Lab Chip*, 2022, **22**, 4593–4602.

131 W. W. Du, Z. K. Li, Y. L. Zhao, X. Zhang, L. L. Pang, W. Wang, T. Jiang, A. F. Yu and J. Y. Zhai, *Chem. Eng. J.*, 2022, **446**, 137268.

132 Q. Gao, T. Tran, X. J. Liao, S. Rosenfeldt, C. Gao, H. Q. Hou, M. Retsch, S. Agarwal and A. Greiner, *ACS Appl. Mater. Interfaces*, 2022, **14**, 19918–19927.

133 H. W. Li, K. J. Wu, Z. Y. Xu, Z. W. Wang, Y. C. Meng and L. Q. Li, *ACS Appl. Mater. Interfaces*, 2018, **10**, 20826–20834.

134 Y. Y. Pei, X. L. Zhang, Z. Y. Hui, J. Y. Zhou, X. Huang, G. Z. Sun and W. Huang, *ACS Nano*, 2021, **15**, 3996–4017.

135 J. N. Wang, X. Y. Yue, X. T. Li, J. Dong, Q. H. Zhang and X. Zhao, *ACS Appl. Polym. Mater.*, 2022, **4**, 3205–3216.



136 C. Liu, L. Xu, L. Y. Kong, Y. Q. Xu, W. Zhou, Q. P. Qiang, L. L. Tian, W. B. Chen, M. S. Cai, T. C. Lang, T. Han and B. T. Liu, *J. Mater. Chem. C*, 2022, **10**, 13064–13073.

137 Y. N. Ma, Y. F. Cheng, J. Wang, S. Fu, M. J. Zhou, Y. Yang, B. W. Li, X. Zhang and C. W. Nan, *InfoMat*, 2022, **4**, e12328.

138 C. J. Park, M. S. Choi, S. H. Lee, H. Kim, T. Lee, M. M. Billah, B. Jung and J. Jang, *Nanomater*, 2022, **12**, 2127.

139 X. M. Wang, Y. J. Chai, Z. P. Wang, J. B. Yu, X. P. Chen and C. P. Wong, *ACS Appl. Mater. Interfaces*, 2021, **9**, 2101663.

140 S. F. Zhao, W. B. Ran, D. P. Wang, R. Y. Yin, Y. X. Yan, K. Jiang, Z. Lou and G. Z. Shen, *ACS Appl. Mater. Interfaces*, 2020, **12**, 32023–32030.

141 S. Sharma, A. Chhetry, M. Sharifuzzaman, H. Yoon and J. Y. Park, *ACS Appl. Mater. Interfaces*, 2020, **12**, 22212–22224.

142 Y. P. Sun, H. L. Tai, Z. Yuan, Z. H. Duan, Q. Huang and Y. D. Jiang, *Part. Part. Syst. Charact.*, 2021, **38**, 2100019.

143 C. M. Boutry, A. Nguyen, Q. O. Lawal, A. Chortos, S. Rondeau-Gagne and Z. N. Bao, *Adv. Mater.*, 2015, **27**, 6954–6961.

144 O. Atalay, A. Atalay, J. Gafford and C. Walsh, *Adv. Mater. Technol.*, 2018, **3**, 1700237.

145 H. Jang, H. Yoon, Y. Ko, J. Choi, S. S. Lee, I. Jeon, J. H. Kim and H. Kim, *Nanoscale*, 2016, **8**, 5667.

146 Y. J. Guo, S. Gao, W. J. Yue, C. W. Zhang and Y. Li, *ACS Appl. Mater. Interfaces*, 2019, **11**, 48594–48603.

147 L. Q. Ma, X. T. Shuai, Y. G. Hu, X. W. Liang, P. L. Zhu, R. Sun and C. P. Wong, *J. Mater. Chem. C*, 2018, **6**, 13232.

148 S. W. Park, P. S. Das, A. Chhetry and J. Y. Park, *IEEE Sens. J.*, 2017, **17**, 6558–6564.

149 Y. S. Luo, J. Y. Shao, S. R. Chen, X. L. Chen, H. M. Tian, X. M. Li, L. Wang, D. R. Wang and B. H. Lu, *ACS Appl. Mater. Interfaces*, 2019, **11**, 17796–17803.

150 G. Z. Wu, M. P. Sarmad, X. L. Xiao, F. C. Ding, K. Dong and X. L. Hou, *Composites, Part A*, 2021, **145**, 106373.

151 C. Mahata, H. Algadi, J. Lee, S. J. Kim and T. Lee, *Measurement*, 2020, **151**, 107095.

152 C. M. Boutry, Y. Kaizawa, B. C. Schroeder, A. Chortos, A. Legrand, Z. Wang, J. Chang, P. Fox and Z. N. Bao, *Nat. Electron.*, 2018, **1**, 314–321.

153 S. M. Lee, R. Hinchet, Y. Lee, Y. Yang, Z. H. Lin, G. Ardila, L. Montes, M. Mouis and Z. L. Wang, *Adv. Funct. Mater.*, 2014, **24**, 1163–1168.

154 X. D. Chen, D. ben Yang, Y. D. Jiang, Z. M. Wu, D. Li, F. J. Gou and J. de Yang, *Sens. Actuators, A*, 1998, **65**, 194.

155 G. H. Haertling, *J. Am. Ceram. Soc.*, 2004, **82**, 797.

156 S. Sharma, R. Singh, T. C. Goel and S. Chandra, *Comput. Mater. Sci.*, 2006, **37**, 86.

157 P. Martins, A. C. Lopes and S. Lanceros-Mendez, *Prog. Polym. Sci.*, 2014, **39**, 683.

158 L. Y. Han, W. Zeng, Y. Dong, X. H. Wang and L. W. Lin, *Adv. Electron. Mater.*, 2022, **8**, 2200012.

159 Y. J. Shi, K. J. Zhang, S. Ding, Z. Y. Li, Y. H. Huang, Y. C. Pi, D. Z. Zhao, Y. W. Zhang, R. K. Wang, B. P. Zhou, Z. X. Yang and J. W. Zhong, *Nano Res.*, 2022, **16**, 1269–1276.

160 Q. Zhong, J. Zhong, X. Cheng, X. Yao, B. Wang, W. Li, N. Wu, K. Liu, B. Hu and J. Zhou, *Adv. Mater.*, 2015, **27**, 7130.

161 A. K. Kalyani, K. Brajesh, A. Senyshyn and R. Ranjan, *Appl. Phys. Lett.*, 2014, **104**, 252906.

162 S. Zhang, R. Xia, T. R. Shrout, G. Zang and J. Wang, *Solid State Commun.*, 2007, **141**, 675.

163 D. Mishra and Y. E. Pak, *European Journal of Mechanics, A: Solids*, 2017, **61**, 279.

164 I. L. Guy, S. Muensit and E. M. Goldys, *Appl. Phys. Lett.*, 1999, **75**, 4133.

165 Y. Chu, J. W. Zhong, H. L. Liu, Y. Ma, N. Liu, Y. Song, J. M. Liang, Z. C. Shao, Y. Sun, Y. Dong, X. H. Wang and L. W. Lin, *Adv. Funct. Mater.*, 2018, **28**, 1803413.

166 P. Samartkit, S. Pullteap and O. Bernal, *Measurement*, 2022, **196**, 111211.

167 N. I. Kim, J. Chen, W. J. Wang, M. Moradnia, S. Pouladi, M. K. Kwon, J. Y. Kim, X. H. Li and J. H. Ryou, *Adv. Funct. Mater.*, 2021, **31**, 2008242.

168 C. F. Lü, S. Wu, B. W. Lu, Y. Y. Zhang, Y. K. Du and X. Feng, *J. Micromech. Microeng.*, 2018, **28**, 025010.

169 P. Fang, X. C. Ma, X. X. Li, X. L. Qiu, R. Gerhard, X. Q. Zhang and G. L. Li, *IEEE Sens. J.*, 2018, **18**, 401–412.

170 Y. F. Zhang, G. P. Lu, M. Chen, Y. R. Liu and R. H. Yao, *IEEE Sens. J.*, 2022, **22**, 12613–12621.

171 H. Lei, Y. F. Chen, Z. Q. Gao, Z. Wen and X. H. Sun, *J. Mater. Chem. A*, 2021, **9**, 20100.

172 Y. B. Zheng, R. W. Omar, Z. P. Hu, T. Duong, J. Wang and H. Haick, *ACS Biomater. Sci. Eng.*, 2021, DOI: [10.1021/acsbiomaterials.1c01106](https://doi.org/10.1021/acsbiomaterials.1c01106), Special issue.

173 Q. Yi, X. C. Pei, P. Das, H. T. Qin, S. W. Lee and R. Esfandyarpour, *Nano Energy*, 2022, **101**, 107511.

174 Y. F. Yu, Y. Y. Feng, F. Liu, H. Wang, H. T. Yu, K. Dai, G. Q. Zheng and W. Feng, *Small*, 2022, 2204365.

175 Y. S. Fang, Y. J. Zou, J. Xu, G. R. Chen, Y. H. Zhou, W. L. Deng, X. Zhao, M. Roustaei, T. K. Hsiao and J. Chen, *Adv. Mater.*, 2021, **33**, 2104178.

176 M. N. Lou, I. Abdalla, M. M. Zhu, X. D. Wei, J. Y. Yu, Z. L. Li and B. Ding, *ACS Appl. Mater. Interfaces*, 2020, **12**, 19965–19973.

177 W. J. Fan, Q. He, K. Y. Meng, X. L. Tan, Z. H. Zhou, G. Q. Zhang, J. Yang and Z. L. Wang, *Sci. Adv.*, 2020, **6**, eaay2840.

178 S. Y. Kim, S. Jang, K. N. Kim, S. Lee, H. Chang, S. Yim, W. Song, S. Lee, J. Lim and S. Myung, *ACS Appl. Nano Mater.*, 2022, **5**, 15192–15200.

179 Z. P. Zheng, D. Yu, B. Q. Wang and Y. P. Guo, *Chem. Eng. J.*, 2022, **446**, 137393.

180 F. F. Gao, X. Zhao, Z. Zhang, L. L. An, L. X. Xu, X. C. Xun, B. Zhao, T. Ouyang, Y. Zhang, Q. L. Liao and L. Wang, *Nano Energy*, 2022, **91**, 106695.

181 Y. E. Shin, Y. J. Park, S. K. Ghosh, Y. Lee, J. Park and H. Ko, *Adv. Sci.*, 2022, **9**, 2105423.

182 H. Lei, J. Xiao, Y. F. Chen, J. W. Jiang, R. J. Xu, Z. Wen, B. Dong and X. H. Sun, *Nano Energy*, 2022, **91**, 106670.

183 M. M. Zhu, M. N. Lou, J. Y. Yu, Z. L. Li and B. Ding, *Nano Energy*, 2020, **78**, 105208.



184 R. Xu, F. Y. Luo, Z. Y. Zhu, M. T. Li and B. Chen, *ACS Appl. Electron. Mater.*, 2022, **4**, 4051–4060.

185 M. N. Lou, I. Abdalla, M. M. Zhu, J. Y. Yu, Z. L. Li and B. Ding, *ACS Appl. Mater. Interfaces*, 2020, **12**, 1597–1605.

186 T. Li, H. Luo, L. Qin, X. Wang, Z. Xiong, H. Ding, Y. Gu, Z. Liu and T. Zhang, *Small*, 2016, **12**, 5042.

187 Y. Wan, Z. Qiu, Y. Hong, Y. Wang, J. Zhang, Q. Liu, Z. Wu and C. F. Guo, *Adv. Electron. Mater.*, 2018, **4**, 1700586.

188 Y.-Q. Liu, J.-R. Zhang, D.-D. Han, Y.-L. Zhang and H.-B. Sun, *ACS Appl. Mater. Interfaces*, 2019, **11**, 38084.

189 B. C. K. Tee, A. Chortos, R. R. Dunn, G. Schwartz, E. Eason and Z. A. Bao, *Adv. Funct. Mater.*, 2014, **24**, 5427.

190 A. Leber, C. Dong, R. Chandran, T. D. Gupta, N. Bartolomei and F. Sorin, *Nat. Electron.*, 2020, **3**, 316–326.

191 G. Schwartz, B. C. K. Tee, J. Mei, A. L. Appleton, D. H. Kim, H. Wang and Z. Bao, *Nat. Commun.*, 2013, **4**, 1859.

192 L. Persano, C. Dagdeviren, Y. Su, Y. Zhang, S. Girardo, D. Pisignano, Y. Huang and J. A. Rogers, *Nat. Commun.*, 2013, **4**, 1633.

193 L. Shuhai, W. Longfei, F. Xiaolong, W. Zheng, X. Qi, B. Suo, Q. Yong and W. Z. Lin, *Adv. Mater.*, 2017, **29**, 1606346.

194 L. Wang, S. Liu, X. Feng, Q. Xu, S. Bai, L. Zhu, L. Chen, Y. Qin and Z. L. Wang, *ACS Nano*, 2017, **11**, 4859–4865.

195 Z. Zhan, R. Lin, V.-T. Tran, J. An, Y. Wei, H. Du, T. Tran and W. Lu, *ACS Appl. Mater. Interfaces*, 2017, **9**, 37921–37928.

196 A. Rinaldi, A. Tamburano, M. Fortunato and M. S. Sarto, *Sensors*, 2016, **16**, 2148.

197 L.-Q. Tao, K.-N. Zhang, H. Tian, Y. Liu, D.-Y. Wang, Y.-Q. Chen, Y. Yang and T.-L. Ren, *ACS Nano*, 2017, **11**, 8790–8795.

198 C. Lou, S. Wang, T. Liang, C. Pang, L. Huang, M. Run and X. Liu, *Materials*, 2017, **10**, 1068.

199 X. H. Cui, F. L. Huang, X. C. Zhang, P. A. Song, H. Zheng, V. Chevali, H. Wang and Z. G. Xu, *iScience*, 2022, **25**, 104148.

200 X. H. Cui, J. W. Chen, W. Wu, Y. Liu, H. D. Li, Z. G. Xu and Y. T. Zhu, *Nano Energy*, 2022, **95**, 107022.

201 X. H. Cui, Y. Jiang, Z. G. Xu, M. Xi, Y. Jiang, P. A. Song, Y. Zhao and H. Wang, *Composites, Part B*, 2021, **211**, 108641.

202 X. H. Cui, Y. Jiang, L. Hu, M. Cao, H. Y. Xie, X. C. Zhang, F. L. Huang, Z. G. Xu and Y. T. Zhu, *Adv. Mater. Technol.*, 2022, 2200609.

203 D. Y. Park, D. J. Joe, D. H. Kim, H. Park, J. H. Han, C. K. Jeong, H. Park, J. G. Park, B. Joung and K. J. Lee, *Adv. Mater.*, 2017, **29**, 1702308.

